Journal of Sound and Vibration (2001) **239**(2), 335–356
doi:10.1006/jsvi.2000.3205, available online at http://www.idealibrary.com on IDEAL®

NON-LINEAR CORRECTION OF VIBRATION PROTECTION SYSTEM CONTAINING TUNED DYNAMIC ABSORBER

A. M. Veprik and V. I. Babitsky

*Department of Mechanical Engineering, Loughborough University, Loughborough, Leicestershire LE*11 3*TU, England. E-mail: a.veprik@lboro.ac.uk*

(*Received* 6 *August* 1999, *and in final form* 15 *June* 2000)

In this paper, the system of vibration protection containing the tuned dynamic absorber is analyzed. To control the system's extraneous resonant responses without affecting the ability of essential linear vibration suppression at antiresonant frequency, the absolute motion of the absorber is limited by the stops mounted upon the base. The analytical solution relies on the theory of momentary impact and technique of periodic Green functions and is obtained in explicit closed form. The frequency responses of the vibration protection system under harmonic excitation with variable frequency are obtained in terms of impact impulses, magnitudes of fundamental harmonics of motion for the primary and secondary systems and also the forces transmitted to the base. The results of calculations are in good agreement with a numerical simulation, which utilizes the realistic model of visco-elastic collision. Some general concepts of practical design of such a vibration protection system are discussed. In particular, the influences of restitution ratio and clearance value are addressed.

1. INTRODUCTION

The method of dynamic absorption, in general, relies on the attachment of a linear lightly damped single-degree-of-freedom (SDOF) system to the harmonically excited primary structure. It is the simplest case when both the primary and the secondary sub-structures are lightly damped SDOF systems. The frequency response function (FRF) of such a combined two-degree-of-freedom (TDOF) system typically displays two sharp resonant peaks and one deep anti-resonant notch which is located exactly at the partial natural frequency of the secondary sub-structure. The appearance of such a notch is used for the essential suppression of vibration of the primary system caused by a harmonic force with constant frequency.

However, the presence of a modified primary resonance and the occurrence of an additional resonance (typically very close to the position of the antiresonant frequency) detract from the use of a tuned dynamic absorber in applications operating with variable frequency of excitation. The use of the optimized amount of damping in the design of a dynamic absorber results in close control of both resonant responses which are intrinsic to a system; however, the penalty is that the positive feature of vibration suppression at the anti-resonant frequency is breached [1, 2].

An interesting approach to the vibration control of a system equipped by a lightly damped dynamic absorber was proposed in 1928 by Ormondroyd and Den Hartog [1]. In order to avoid resonances in the system containing such a dynamic absorber, they proposed

0022-460X/01/020335 + 22 $35.00/0

to limit the relative motion of the absorber to the primary structure by means of elastic stops. They also suggested designing the sway space of the dynamic absorber in such a manner as to provide impactless linear motions of both masses in the desired vicinity of the anti-resonant frequency. Such a design allows for maintaining the desired feature of linear dynamic suppression of harmonic vibration. As soon as the relative motion of the absorber exceeds the pre-designed clearance (as a result of approaching the excitation frequency of one of the resonant frequencies, in this instance) the stops come into play, thus limiting the relative motion of the absorber. The authors of reference [1] believed that as the stops change the elastic properties of the entire system "no resonance can occur even if no damping exists in the system".† They also indicated that an analytical description of the dynamics of such a system is extremely difficult.

Since then, numerous researchers have been attracted by the simplicity of this elegant engineering solution and have studied such an approach numerically (see, for example, references [3, 4]). To our knowledge, the analytical solution has not yet been obtained.

It is evident that in the case mentioned, the control over the resonances relies entirely on an intensive vibro-impact interaction between the absorber and the primary structure. That may cause excessive dynamic responses and, therefore, damage to the sensitive internal components of the primary structure. As distinct from the model of reference [1], in the present paper the restriction of motion of a dynamic absorber takes place in its absolute motion by means of the stop (bumper) mounted upon the stationary base. Within the framework of such a design, it is possible to correct effectively the dynamic response of the system in the vicinities of both resonances without affecting the positive feature of essential linear vibration suppression at the antiresonant frequency. Since the control of resonant responses relies now on the vibro-impact process between the dynamic absorber and the stationary base, the primary system and its sensitive components may be significantly relieved from the impact dynamic loading.

The authors utilized the theory of momentary impact and technique of *periodic Green functions* (PGF) [5] to study the dynamics of the non-linear vibration protection system under harmonic excitation with variable frequency. The obtained exact analytical expressions describe the time histories of the motions of the primary and secondary systems and also the forces transmitted to the base, and contain a full set of harmonics. The fundamental harmonics are then extracted from the exact solutions and used for representation of correspondent frequency responses.

The results of calculations are in good agreement with a numerical simulation, which relies on the realistic model of visco-elastic collision.

Some general concepts of practical design of such a vibration protection system are discussed. In particular, the influences of restitution ratio and clearance value are addressed.

2. DYNAMIC MODEL AND ANALYTICAL SOLUTION OF VIBRO-IMPACT PROBLEM

Figure 1 shows the dynamic model of the system. The primary system of mass M_1 is suspended from the base by a visco-elastic flexural element which is represented by a parallel combination of spring, K_1, and dashpot, B_1. The absorber of the mass M_2 is attached to the primary system by means of the visco-elastic flexural element which is

†The possibility of the vibro-impact resonance which arise on the right-hand side vicinities of the linear natural frequencies was absolutely ignored by the authors of reference [1]. To prevent the appearance of non-linear (vibro-impact) resonances, a sufficient amount of energy has to be dissipated at collisions with the stops [5].

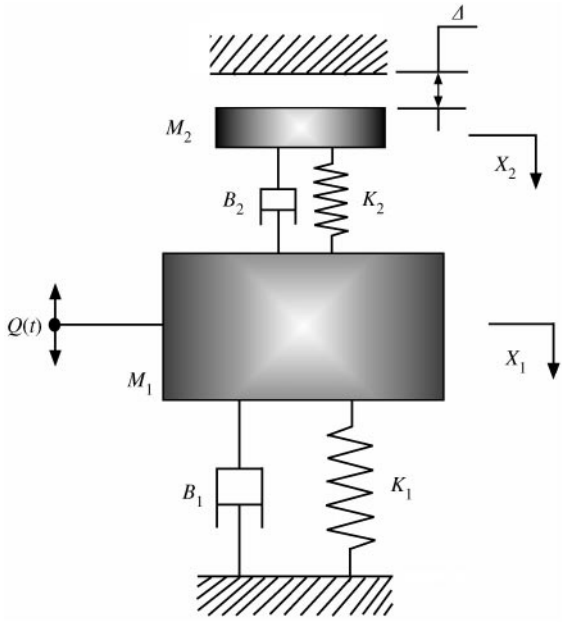

Figure 1. Dynamic model of vibro-impact dynamic absorber.

shown as a parallel combination of the spring, K_2, and the dashpot, B_2. The primary system is subjected to the action of the external force $Q(t) = q \sin \omega t$, where q and ω are the amplitude and angular frequency, respectively. As a result of the excitation, both masses are involved in the absolute motions $X_1(t)$ and $X_2(t)$, as shown in Figure 1. The absolute motion of the secondary mass is limited by a solid stationary stop positioned with a clearance, Δ, with respect to the static equilibrium of the absorber mass. The equations of motion which account for the collision of the secondary sub-system with the stop [5] take the form

$$\begin{aligned} &M_1\ddot{X}_1 + B_1\dot{X}_1 + B_2(\dot{X}_1 - \dot{X}_2) + K_1X_1 + K_2(X_1 - X_2) = Q(t), \\ &M_2\ddot{X}_2 + B_2(\dot{X}_2 - \dot{X}_1) + K_2(X_2 - X_1) + \Phi(X_2, \dot{X}_2) = 0, \end{aligned} \tag{1}$$

where the force of impact interaction $\Phi(X_2, \dot{X}_2)$ is a function of the absolute co-ordinate and velocity of the absorber.

Due to the special choice of the clearance and small damping which is used in the absorber design, the system vibrates linearly (without collisions) for almost the entire frequency span. The only exceptions are in the vicinities of linear resonant frequencies; the phenomenon of non-linear (vibro-impact) resonance takes place to the right of these frequencies [5]. As a result of periodic excitation in the above frequency bands, a steady state non-linear resonant regime with a single-collision per period arises.

The method of PGF is a convenient tool which is well suited for the analysis of such resonant regimes [5, 6]. The force of impact interaction in this regime may be thought of as a periodic function of time $F(t)$ and, generally speaking, may be represented in the form of the Fourier series

$$F(t) = \Phi(X_2, \dot{X}_2) = \sum_{m=-\infty}^{\infty} F_m \exp(jm\omega t), \quad t \in]-\infty, \infty[, \tag{2}$$

where

$$F_m = \frac{1}{T}\int_0^T F(t)\exp(-\mathrm{j}m\omega t)\,\mathrm{d}t, \tag{3}$$

$\mathrm{j} = \sqrt{-1}$ is complex unity, where $T = 2\pi/\omega$ is the period of the process.

By letting $\Phi(X_2, \dot{X}_2) = 0$, the complex dynamic compliances (receptances) of the linear system are obtained from (1) in the form

$$H_{11}(\mathrm{j}\omega) = \frac{(-M_2\omega^2 + \mathrm{j}B_2\omega + K_2)}{D(\mathrm{j}\omega)}, \quad H_{12}(\mathrm{j}\omega) = \frac{(\mathrm{j}B_2\omega + K_2)}{D(\mathrm{j}\omega)},$$
$$H_{22}(\mathrm{j}\omega) = \frac{[-M_1\omega^2 + \mathrm{j}(B_1 + B_2)\omega + K_1 + K_2]}{D(\mathrm{j}\omega)}, \tag{4}$$

$$D(\mathrm{j}\omega) = [-M_1\omega^2 + \mathrm{j}(B_1 + B_2)\omega + K_1 + K_2][-M_2\omega^2 + \mathrm{j}B_2\omega + K_2] - (\mathrm{j}B_2\omega + K_2)^2. \tag{5}$$

For the periodic single-impact process (single-impact over the period T), one finds by means of superposition

$$X_1(t) = q|H_{11}(\mathrm{j}\omega)|\cos[\omega t + \psi_{11}(\omega) + \varphi] - \sum_{m=-\infty}^{\infty} H_{12}(\mathrm{j}m\omega)F_m\exp(\mathrm{j}m\omega t),$$
$$X_2(t) = q|H_{12}(\mathrm{j}\omega)|\cos[\omega t + \psi_{12}(\omega) + \varphi] - \sum_{m=-\infty}^{\infty} H_{22}(\mathrm{j}m\omega)F_m\exp(\mathrm{j}m\omega t), \quad t \in]-\infty, \infty[. \tag{6}$$

The "first terms" on the right-hand sides of both equations (6) represent the steady state solution to a linear problem-impactless motion, where $|H_{11}(\mathrm{j}\omega)|$, $|H_{12}(\mathrm{j}\omega)|$ are the moduli of the dynamic compliances at the frequency ω; $\psi_{11}(\omega)$, $\psi_{12}(\omega)$ are the arguments, and φ is the phase of impact relative to the external force.

The summation terms in both equations (6) represent the "vibro-impact portion" of the solution-the steady state response of the system to the periodic sequence of impact impulses.

Substitution of equation (3) into the summation terms of both equations (6), and changing the sequence of summation and integration yields the non-linear integro-differential equations in the form

$$X_1(t) = q|H_{11}(\mathrm{j}\omega)|\cos[\omega t + \psi_{11}(\omega) + \varphi] - \int_0^T \chi_{12}(t-\tau)\Phi[x_2(\tau), \dot{x}_2(\tau)]\,\mathrm{d}\tau,$$
$$X_2(t) = q|H_{12}(\mathrm{j}\omega)|\cos[\omega t + \psi_{12}(\omega) + \varphi] - \int_0^T \chi_{22}(t-\tau)\Phi[x_2(\tau), \dot{x}_2(\tau)]\,\mathrm{d}\tau,$$

where the PGFs $\chi_{12}(t)$, $\chi_{22}(t)$, are defined as follows [5]:

$$\chi_{12}(t) = \frac{1}{T}\sum_{m=-\infty}^{\infty} H_{12}(\mathrm{j}m\omega)\exp(\mathrm{j}m\omega t), \quad \chi_{22}(t) = \frac{1}{T}\sum_{m=-\infty}^{\infty} H_{22}(\mathrm{j}m\omega)\exp(\mathrm{j}m\omega t),$$
$$t \in]-\infty, \infty[. \tag{7}$$

The duration of impact is typically very small as compared with the period T. Therefore, with the use of the mean-value theorem, one obtains the two-parametric representation of the desired solution in terms of unknown impulse of impact force J and phase φ:

$$X_1(t) = q|H_{11}(j\omega)|\cos[\omega t + \psi_{11}(\omega) + \varphi] - J\chi_{12}(t),$$

$$X_2(t) = q|H_{12}(j\omega)|\cos[\omega t + \psi_{12}(\omega) + \varphi] - J\chi_{22}(t), \tag{8}$$

where $t \in]-\infty, \infty[$ and

$$J = \int_0^T \Phi[X_2(\tau), \dot{X}_2(\tau)]\,d\tau.$$

For the momentary impact [5], the impulse of impact force may be expressed through the restitution ratio, R, and the pre-impact velocity, $\dot{X}_2(-0)$: that is

$$J = M_2(1 + R)\dot{X}_2(-0). \tag{9}$$

The series (7) are defined in the infinite time interval. To simplify the solution, they may be summed and corresponding PGFs may be found in an explicit form for the finite time interval $[0, T]$ of periodicity [5].

The complex dynamic compliance, $H(j\omega)$, of a lightly damped system with different and well-distanced natural frequencies may be approximated by the eigenform decomposition

$$H(j\omega) \approx \sum_{i=1}^{N} \frac{A_i}{\Omega_i^2 - \omega^2 + 2j\xi_i\Omega_i\omega}, \tag{10}$$

where N is the number of relevant degrees of freedom ($N = 2$, in this instance), and Ω_i, ξ_i, A_i are undamped natural frequencies, loss factors and form factors, respectively. From equation (5), by letting $B_{1,2} = 0$, the natural undamped frequencies $\Omega_{1,2}$ are found as the roots of the equation $D(j\omega) = 0$; these are

$$\Omega_{1,2} = \sqrt{\frac{(K_1M_1 + K_1M_2 \to K_2M_1) \pm \sqrt{(K_1M_1 + K_1M_2 + K_2M_1)^2 - 4K_1K_2M_1M_2}}{2M_1M_2}} \tag{11}$$

The loss factors and the form factors cannot be estimated explicitly for the damped system. In this article, these parameters are obtained approximately from a curve-fitting procedure with expressions (4) and (10) involved.

The complex dynamic compliance in the form (10) yields the closed-form representation of the PGF in the interval of periodicity [5], that is,

$$\chi(t) = \sum_{i=1}^{N} \frac{A e^{-\xi_i\Omega_i t}[\sin\Theta_i t + e^{-\xi_i\Omega_i T}\sin\Theta_i(T - t)]}{\Theta_i(1 + e^{-2\xi_i\Omega_i T} - 2e^{-\xi_i\Omega_i T}\cos\Theta_i T)}, \quad 0 \leqslant t \leqslant T, \tag{12}$$

where the damped natural frequencies are $\Theta_i = \Omega_i\sqrt{1 - \xi_i^2}$, $i = 1, 2$.

The unknown phase and impulse may be obtained from the conditions of impact [5]:

$$X_2(0) = \Delta, \quad J = M_2(1 + R)\dot{X}_2(-0), \quad J \geqslant 0. \tag{13}$$

Substitution of equations (8) into equations (13) yields

$$q|H_{12}(j\omega)|\cos[\varphi + \psi_{12}(\omega)] - J\chi_{22}(0) = \Delta,$$

$$J = (1 + R)M_2[-\omega q|H_{12}(j\omega)|\sin[\varphi + \psi_{12}(\omega)] + J\dot{\chi}_{22}(-0)],$$

where for the lightly damped systems [5]

$$\dot{\chi}_{22}(-0) \approx \frac{1}{2M_2}.$$

In accordance with equation (12) one finds

$$\chi_{22}(0) = \sum_{i=1}^{N} \frac{A_i e^{-\xi_i \Omega_i t} \sin \Theta_i T}{\Theta_i (1 + e^{-2\xi_i \Omega_i T} - 2e^{-\xi_i \Omega_i T} \cos \Theta_i T)}, \quad 0 \leqslant t \leqslant T, \tag{14}$$

where the natural undamped frequencies $\Omega_{1,2}$ are derived from equation (11) and modal parameters A_i, ξ_i are obtained from eigenform decomposition of the complex compliance $H_{22}(j\omega)$ (see equation (4)) in the form (10).

From the conditions of impact, one has two equations in the unknown phase $\phi = \varphi + \psi_{12}(\omega)$ and impulse J:

$$\sin \phi = -\frac{J(1 - R)}{2(1 + R)M_2 \omega q|H_{12}(j\omega)|}, \quad \cos \phi = \frac{\Delta + J\chi_{22}(0)}{q|H_{12}(j\omega)|}. \tag{15}$$

Eliminating the phase ϕ, one readily finds for the impact impulse

$$J(\omega) =$$

$$= \frac{-\Delta\chi_{22}(0) \pm \sqrt{[\Delta\chi_{22}(0)]^2 - [((1-R)/2(1+R)M_2\omega)^2 + \chi_{22}^2(0)][\Delta^2 - |H_{12}(j\omega)|^2 q^2]}}{[((1-R)/2(1+R)M_2\omega)^2 + \chi_{22}^2(0)]}. \tag{16}$$

The analysis of stability which was conducted in reference [5] indicates that a stable regime corresponds to the positive sign in equation (16). From reference [5], the obvious conditions of vibroimpact regime existence are as follows:

$$|\sin \phi| \leqslant 1, \quad J \geqslant 0.$$

The substitution of the estimated values for the impulse J and phase ϕ back into equations (8) yields the closed-form explicit solution describing the periodic forced vibration of the TDOF system with collisions under the harmonic excitation of arbitrary frequency.

3. ANALYSIS OF FUNDAMENTAL HARMONICS AND IMPACT IMPULSES

The main concerns in an analysis of a vibration protection system which relies on a dynamic absorber are the dynamic components of (i) accelerations and deflections of the primary and secondary systems, and (ii) the force transmitted to the base.

Since a momentary impact model has been assumed, it is impossible to estimate the peak values of impact forces and accelerations (these take infinite values at the moment of collision).

As the systems under consideration are well-pronounced low-pass filters, the first harmonics give good representation of the entire process [5]. Therefore, one can perform an analysis of the corresponding frequency responses in terms of the fundamental harmonics, which are extracted from the above exact solutions. Numerical simulations validate this approach.

Since the values of phase and impulse have already been obtained from equations (15) and (16) one call readily calculate the fundamental harmonics of the processes (8)

$$\mathscr{F}^{(1)}[X_1(t)] = q|H_{11}(\mathrm{j}\omega)|\cos[\omega t + \psi_{11}(\omega) + \varphi] - \frac{2J}{T}|H_{12}(\mathrm{j}\omega)|\cos[\omega t + \psi_{12}(\omega)], \quad (17)$$

$$\mathscr{F}^{(1)}[X_2(t)] = q|H_{12}(\mathrm{j}\omega)|\cos[\omega t + \psi_{12}(\omega) + \varphi] - \frac{2J}{T}|H_{22}(\mathrm{j}\omega)|\cos[\omega t + \psi_{22}(\omega)]. \quad (18)$$

The magnitudes of the fundamental harmonics $|\mathscr{F}^{(1)}[X_{1,2}]|$ may be calculated readily from equations (17) and (18).

The force which is transmitted to the base may be represented in the form

$$F(t) = F_s(t) + F_i(t),$$

where

$$F_s(t) = K_1 X_1(t) + B_1 \dot{X}_1(t) \quad (19)$$

is the force transmitted through the flexural suspension and

$$F_i(t) = J\delta^{\mathrm{T}}(t) \quad (20)$$

is the force transmitted through impacts.

The fundamental harmonic of the force transmitted through flexural suspension is calculated with the help of equations (17) and (19):

$$\begin{aligned}\mathscr{F}^{(1)}[F_s(t)] &= K_1\mathscr{F}^{(1)}[X_1(t)] + B_1\mathscr{F}^{(1)}[\dot{X}_1(t)] = \\ &= K_1\left\{q|H_{11}(\mathrm{j}\omega)|\cos[\omega t + \psi_{11}(\omega) + \varphi] - \frac{2J}{T}|H_{12}(\mathrm{j}\omega)|\cos[\omega t + \psi_{12}(\omega)]\right\} + \\ &+ B_1\left\{-q\omega|H_{11}(\mathrm{j}\omega)|\sin[\omega t + \psi_{11}(\omega) + \varphi] + \right. \\ &\left. + \frac{2J\omega}{T}|H_{12}(\mathrm{j}\omega)|\sin[\omega t + \psi_{12}(\omega)]\right\}. \end{aligned} \quad (21)$$

The fundamental harmonic of the force transmitted through impact is obtained with the help of equation (20):

$$\mathscr{F}^{(1)}[F_i(t)] = \frac{2J}{T}\cos\omega t. \quad (22)$$

With the use of equations (21) and (22), the fundamental harmonic of the resultant force is

$$\mathscr{F}^{(1)}[F(t)] = K_1 \left\{ q|H_{11}(j\omega)| \cos[\omega t + \psi_{11}(\omega) + \varphi] - \frac{2J}{T}|H_{12}(j\omega)| \cos[\omega t + \psi_{12}(\omega)] \right\} +$$

$$+ B_1 \left\{ -q\omega|H_{11}(j\omega)| \sin[\omega t + \psi_{11}(\omega) + \varphi] + \right.$$

$$\left. + \frac{2J\omega}{T}|H_{12}(j\omega)| \sin[\omega t + \psi_{12}(\omega)] \right\} + \frac{2J}{T} \cos \omega t. \tag{23}$$

From equation (23), the magnitude of the fundamental harmonic of the force transmitted to the base $|\mathscr{F}^{(1)}[F]|$ may be readily estimated.

4. NUMERICAL EXAMPLE AND DISCUSSION

The parameters for the numerical example were taken as follows:

$$M_1 = 1\,\text{kg}, \quad M_2 = 0{\cdot}1\,\text{kg}, \quad K_1 = 25\,000\,\text{N/m}, \quad K_2 = 4300\,\text{N/m}, \quad B_1 = 0{\cdot}8\,\text{kg/s},$$

$$B_2 = 0{\cdot}08\,\text{kg/s}, \quad q = 10\,\text{N}, \quad \Delta = 3\,\text{mm}. \tag{24}$$

First, one can consider as a reference the linear case at $\Delta \to \infty$.

Figure 2 shows the superimposed magnitudes of the fundamental harmonics of displacement of the primary and secondary mass against frequency. It is seen that linear resonances take place at the frequencies 23 and 36 Hz, where the magnitudes attain large values. The anti-resonant frequency of the primary mass is 33 Hz, where the dynamic response becomes negligible.

Figure 3 depicts the magnitude of the fundamental harmonic of the force transmitted to the base through the suspension of the primary system (impacts are absent in this case) against frequency. It is seen that in the vicinities of linear responses of 23 and 36 Hz essential force transmission takes place, and in the vicinity of linear anti-resonance (33 Hz) the force transmission becomes negligible.

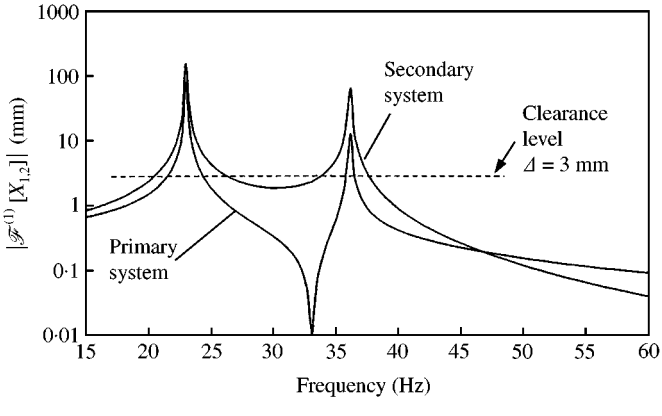

Figure 2. Frequency responses (displacements of the primary and secondary systems) in the linear case ($\Delta \to \infty$).

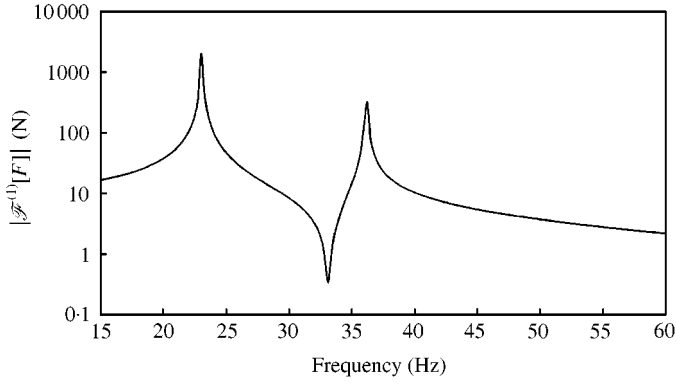

Figure 3. Frequency response (force transmitted to the base) in the linear case ($\Delta \to \infty$).

It is important now to recall that it is desirable to control the resonant responses of the system and to keep the linear anti-resonance response unaffected. From Figure 2, the response of the secondary system at anti-resonance is 2·27 mm. The choice of the clearance $\Delta = 3$ mm (see Figure 2) allows the impactless motion of the secondary system in a sufficient frequency band, which is 27–34 Hz.

The modal parameters Ω_i, ξ_i, A_i are required now for calculation of $\chi_{22}(0)$ in accordance with expression (14). The undamped natural frequencies $\Omega_{1,2}$ are obtained for the numerical values of equations (24) from equation (11); these are

$$\frac{\Omega_1}{2\pi} = 23{\cdot}02 \text{ Hz}, \quad \frac{\Omega_2}{2\pi} = 36{\cdot}07 \text{ Hz}. \tag{25}$$

The complex compliance $H_{22}(j\omega)$ from equation (4) was approximated by the eigenform decomposition (10). The following modal parameters were estimated from curve-fitting (the numerical values of equations (24) were used):

$$A_1 = 2{\cdot}75, \quad A_2 = 7{\cdot}25, \quad \xi_1 = 0{\cdot}0022, \quad \xi_2 = 0{\cdot}0023. \tag{26}$$

Figure 4 shows the modulus of the complex compliance $|H_{22}(j\omega)|$ which is calculated firstly in accordance with equation (4) with numerical parameters (24) (——) and secondly in accordance with equation (10) (○) with numerical values (25) and (26).

Figures 5 and 6 show the magnitudes of the fundamental harmonics (formulae (17) and (18)) of the secondary and primary masses against excitation frequency at different restitution ratios R (see the legends). The corresponding linear response of the system (labelled as LIN, see the legend) is superimposed for reference. The dynamic responses of both secondary and primary systems show the distortion and essential suppression (as compared with the linear case) in the vicinities of the linear resonances. This is due to the violation of the conditions of linear resonance and caused by the interaction of the secondary system with the obstacle. At the same time, the presence of the obstacle causes the development of non-linear (vibro-impact) resonances pulled well to the right of the frequencies of linear resonance (see the footnote of the Introduction). At the frequencies of vibro-impact resonance, the magnitudes of the fundamental harmonic may be even higher than that in the linear case. An implementation of sufficient damping into the contact zone is, therefore, a must for the close control of vibro-impact resonance. From Figures 5 and 6, the decrease in the value of the restitution ratio, R, results in the narrowing of the frequency band of the existence of vibro-impact resonance and also in a reduction of the peak value of

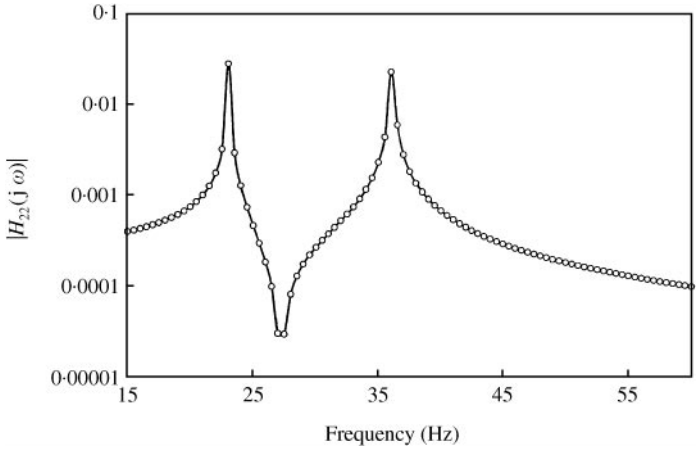

Figure 4. Accuracy of curvefitting.

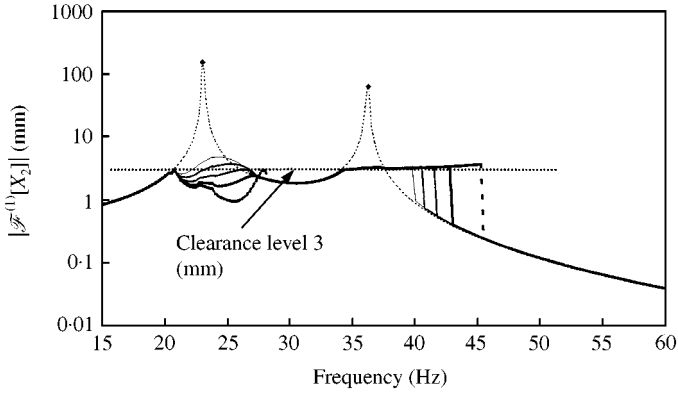

Figure 5. Frequency response (fundamental harmonic of displacement of the secondary system) in the vibro-impact case ($\Delta = 3$ mm) at different restitution ratios: ·····, LIN; —— -0; ——, $-0{\cdot}2$; ————, $-0{\cdot}4$; ————, $-0{\cdot}6$; - - -, $-0{\cdot}8$.

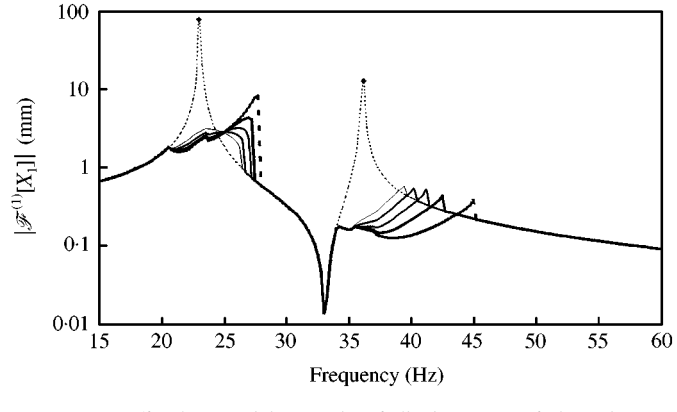

Figure 6. Frequency response (fundamental harmonic of displacement of the primary system in the case ($\Delta = 3$ mm) at different restitution ratios: ·····, LIN; —— -0; ——, $-0{\cdot}2$; ————, $-0{\cdot}4$; ————, $-0{\cdot}6$; - - -, $-0{\cdot}8$.

response. It is obvious from these figures that for the better correction of the frequency response, the lowest value of the restitution ratio is preferable.

The latter is of particular importance for the primary system, since vibration control of the primary system is our main objective. For example, at the restitution ratio $R = 0{\cdot}2$ one obtains the suppression of the dynamic responses in the vicinity of the first and second resonances by factors of 28 and 23 respectively. At the same time, the portion of the frequency response in the frequency band 27–34 Hz (see Figures 2, 5 and 6) which contains the deep anti-resonant notch remains unaffected.

Figure 7 shows the magnitude of the fundamental harmonic of the force transmitted to the base through the primary suspension and impact (formula (21) was used), against excitation frequency at different restitution ratios R (see the legend). The corresponding graph representing the force transmission in the linear case (labelled as LIN, see the legend) is superimposed for reference.

From Figure 7, the essential control of the force transmitted to the base takes place in spite of the impacts. The force transmission at the first and second resonances was decreased in the case of $R = 0{\cdot}2$ by factors of 25 and 30 respectively.

It is of particular interest to analyze in Figure 8 the dependencies of the impact impulse against the frequency at different restitution ratios (see the legend). This graph shows the

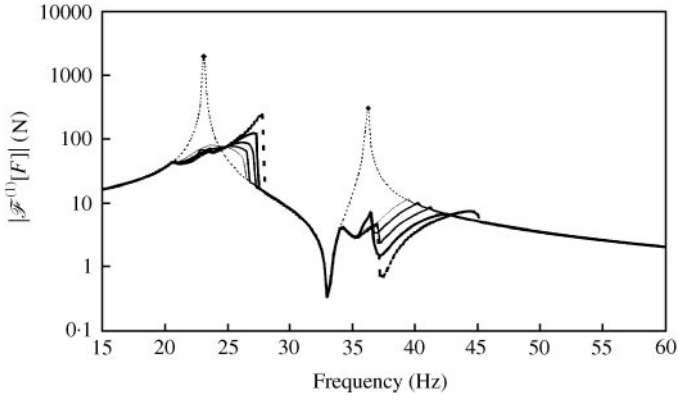

Figure 7. Frequency response (fundamental harmonic of force transmitted to the base) of the primary system in the vibro-impact case ($\Delta = 3$ mm) at different restitution ratios: ·····, LIN; —— -0; ——, $-0{\cdot}2$; ——, $-0{\cdot}4$; ——, $-0{\cdot}6$; - - -, $-0{\cdot}8$.

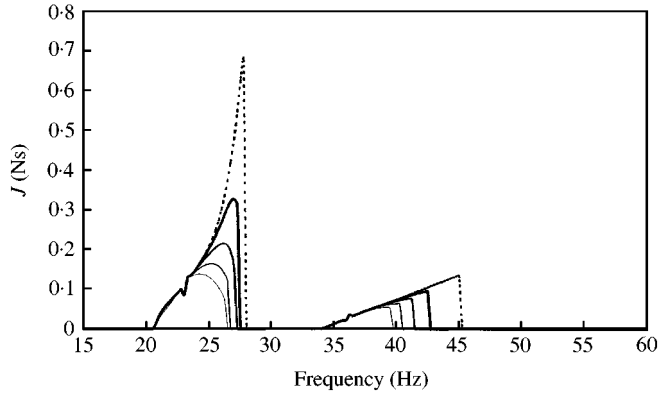

Figure 8. Frequency response (impact impulse) in the vibro-impact case ($\Delta = 3$ mm) at different restitution ratios: —— -0; ——, $-0{\cdot}6$; ——, $-0{\cdot}4$; ——, $-0{\cdot}2$; - - -, $-0{\cdot}0$.

frequency bands of existence of vibro-impact regimes, the character of frequency pulling and change in intensity of vibro-impact processes at different restitution ratios. The calculations were performed in accordance with formula (16). The values of full impact impulses are used for the estimation of the peak accelerations.

5. NUMERICAL SIMULATION

5.1. DYNAMIC MODEL

The present simulation is based on the realistic model of non-momentary visco-elastic collision suggested by the authors in references [5–7]. Such a model is required here to produce a reference solution containing the peak values of impact forces and impulses.

In Figure 9, the dynamic model of the system is represented. This model is identical to that shown in Figure 1 with the exception that the motion of the secondary mass is limited by the compliant visco-elastic bumper, which is modelled as a parallel combination of the linear spring, K, and the dashpot, B.

The equations of motion accounting for the collisions of the secondary system against the bumper take the form of equations (1), where, as above, the threshold force of impact interaction $\Phi(X_2, \dot{X}_2)$ is a function of co-ordinate and velocity and takes the form [5–7]

$$\Phi(X_2, \dot{X}_2) = \begin{cases} K(X_2 - \Delta) + B\dot{X}_2 & \text{if} \quad X_2 \geqslant \Delta \quad \text{and} \quad \Phi(X_2, \dot{X}_2) > 0 \\ 0 & \text{if} \quad X_2 \geqslant \Delta \quad \text{and} \quad \Phi(X_2, \dot{X}_2) \leqslant 0 \\ 0 & \text{if} \quad X_2 < \Delta \end{cases} \tag{25}$$

5.2. SIMULINK DIAGRAM

The system in Figure 9 is "subjected" to the direct swept sine test. Figure 10 portrays the corresponding Simulink diagram.

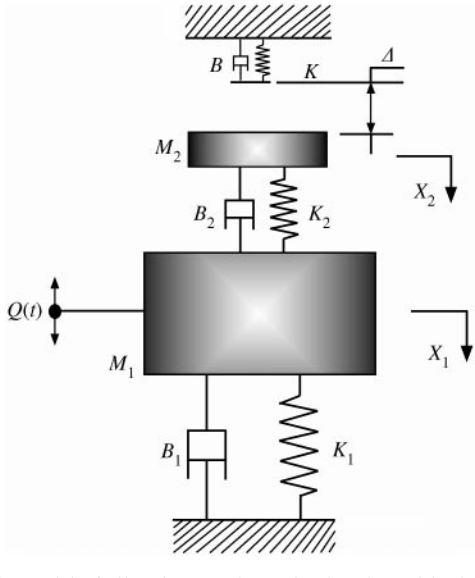

Figure 9. Dynamic model of vibro-impact dynamic absorber with visco-elastic bumper.

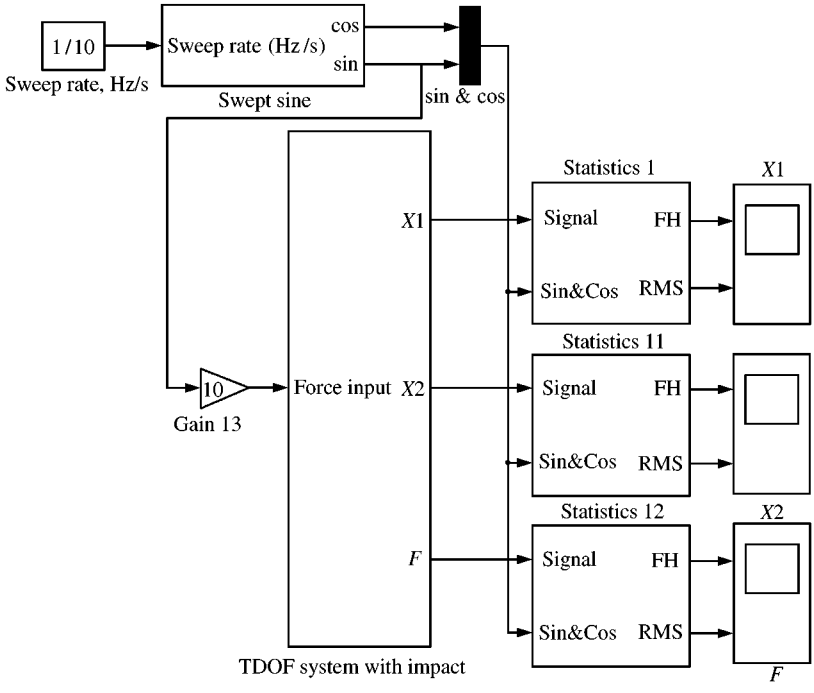

Figure 10. Simulink diagram.

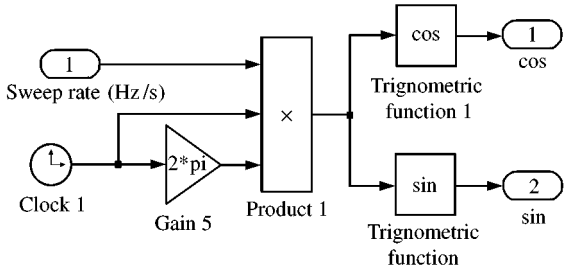

Figure 11. Sub-system "Swept sine".

In Figure 11, the subsystem "Swept sine" produces two signals, these are $\sin \omega t$ and $\cos \omega t$ with linearly varying frequency $\omega = \omega(t) = 2\pi\alpha t$, where α is a sweep rate, Hz/s. These signals are required for the current calculation of the fundamentals harmonics of the processes. Simultaneously, one of these signals is used to evaluate the excitation signal $q \sin \omega t$, which is fed to the input of the subsystem "TDOF System with Impact" performing a calculation of the displacements of the primary and secondary system and of the force transmitted to the base (X1, X2, F, as shown in Figure 10). Figure 12 shows the internal structure of the above subsystem. It contains the diagram for simulation of the linear part of the TDOF system and non-linear block "Impact Force" (see Figure 12) which performs the transformation of the displacement and velocity of the secondary system into the impact force in accordance with formula (25). In this diagram, the lower limit in the "Dead Zone" block is set as $-\infty$. The block "Relational Operator"

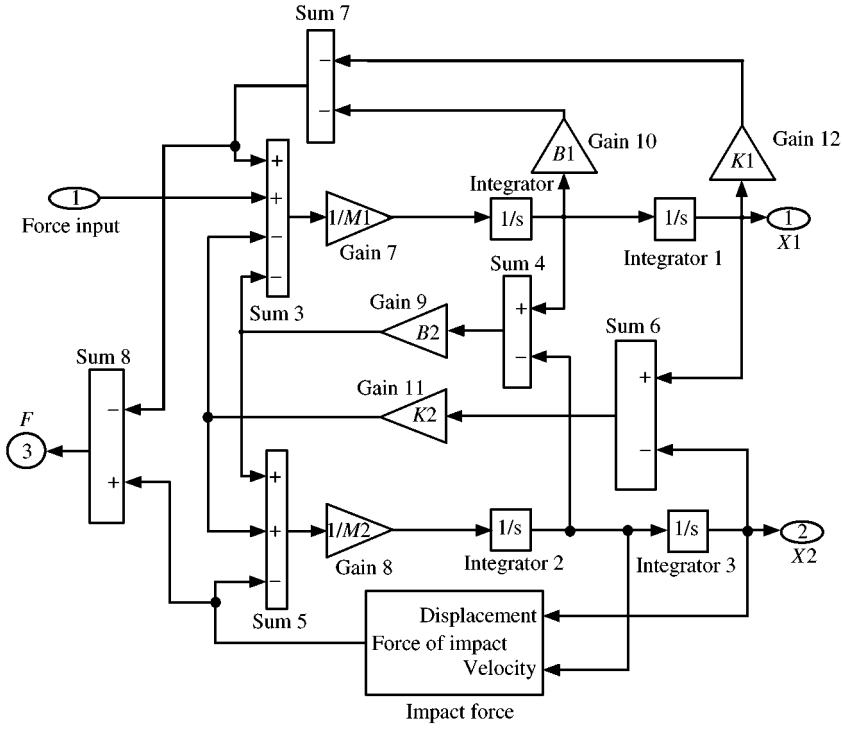

Figure 12. Sub-system "TDOF System with Impact".

produces unity if displacement and impact force are of the same polarity and null otherwise.

The signals obtained (displacements and force transmitted to the base) (see Figure 10), are then fed to the "Statistics" blocks which calculate the current value of the fundamental harmonic (FH) and root mean square (RMS) of the corresponding signals. The internal structure of these blocks is shown in Figures 13 and 14.

By using the diagram of Figure 13, one can simulate the dynamic response of the mechanical system in terms of fundamental harmonics and RMS levels. This gives the opportunity to make a general assessment of the accuracy of theoretical analysis which relies on the method of PGFs.

5.3. RESULTS OF SIMULATION AND DISCUSSION

One can compare the results with those of the analytical solution obtained by means of the PGF method in the case of the restitution ratio $R = 0{\cdot}2$. For this purpose one considers, as above, the mechanical system with parameters (24).

It is convenient [7] to express the elastic and damping properties of the bumper in terms of the apparent natural frequency $\Omega_b = \sqrt{K/M_2}$ and the apparent loss factor $\xi_b = B/2M_2\Omega_b$. It is important to note that the dynamic system with such parameters exists during the short time of impact only.

In these notations the expressions for the bumper stiffness and damping take the forms $K = M_2\Omega_b^2$, $B = 2M_2\xi_b\Omega_b$.

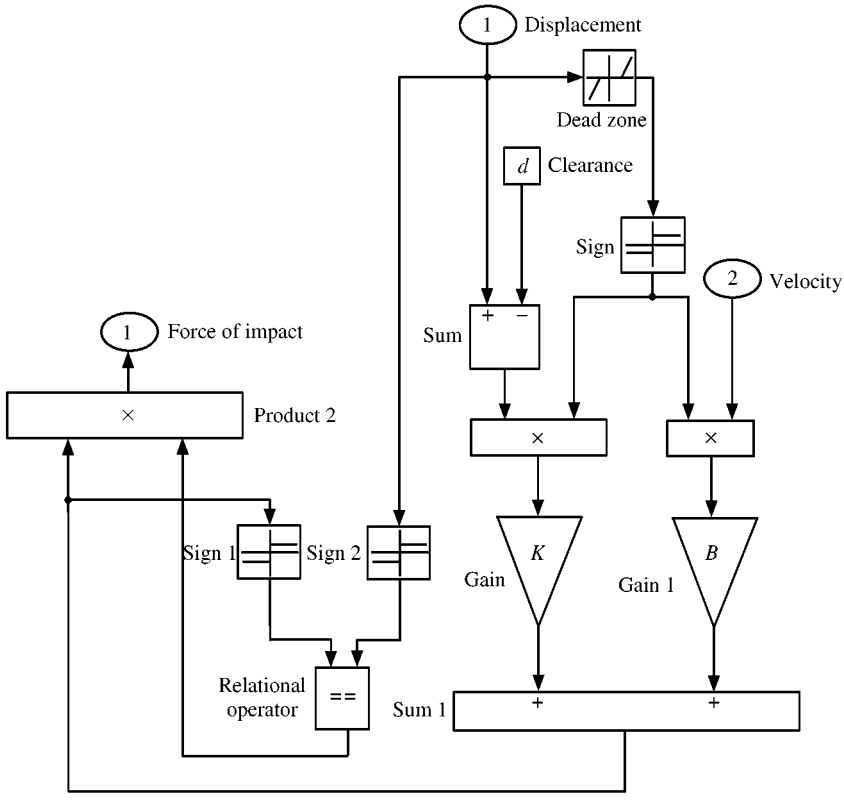

Figure 13. Sub-system "Impact Force".

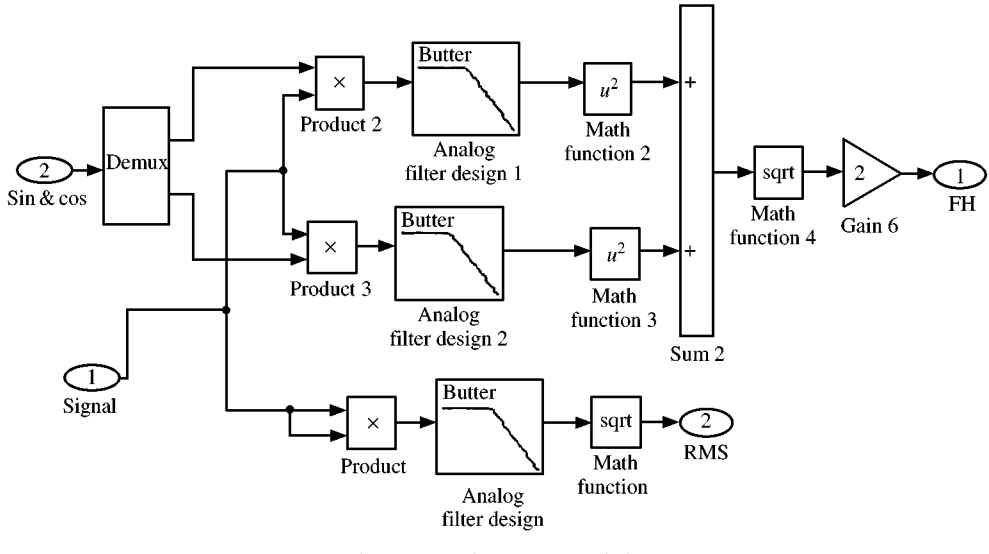

Figure 14. Sub-system "Statistics".

From reference [5], at visco-elastic impact the restitution ratio is a function of the loss factor only,

$$R(\xi_b) = -\exp\left[-\frac{\xi_b}{\sqrt{1-\xi_b^2}}\operatorname{atan}\left(-\frac{2\xi_b\sqrt{1-\xi_b^2}}{1-2\xi_b^2}\right)\right]\sin\left[\operatorname{atan}\left(-\frac{2\xi_b\sqrt{1-\xi_b^2}}{1-2\xi_b^2}\right)\right], \quad (26)$$

as Figure 15 shows. From Figure 15, the loss factor $\xi_b = 0{\cdot}65$ corresponds to the restitution ratio $R = 0{\cdot}2$ (this point is labelled as ◆). For the purpose of numerical simulation $\Omega_b/2\pi = 250$ Hz. The sweep rate is taken as $\alpha = 0{\cdot}1$ Hz/s.

Figures 16 and 17 show the superimposed frequency responses of the primary and of secondary systems in terms of overall RMS levels and the RMS level of the fundamental harmonics. The entire process is well represented by the fundamental harmonic. This particularly holds true for the primary system: the influence of impacts resulting in a singularity which is represented in the motion of the secondary system is not seen in the motion of the primary system due to the filtering feature [5].

Figures 18–20 show the magnitudes of fundamental harmonics of the primary and secondary systems and the force transmitted to the base, and also compare these with the corresponding responses of the linear system (3). These plots indicate the desired

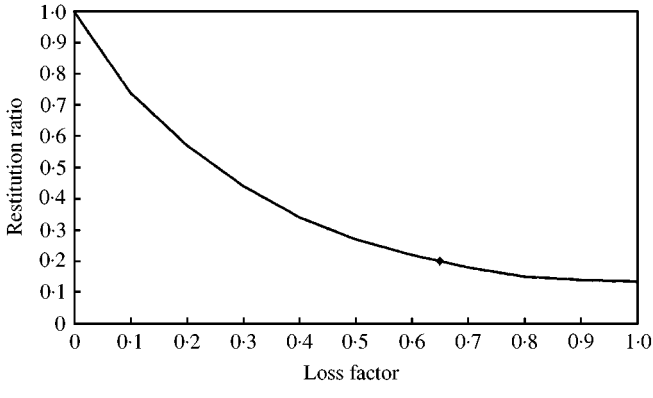

Figure 15. Restitution ratio vs bumper loss factor.

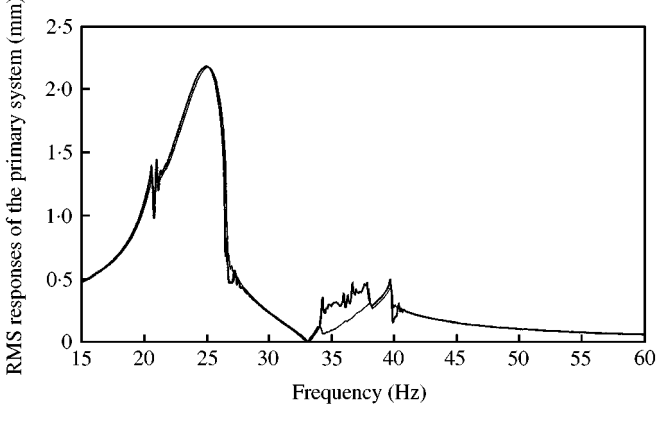

Figure 16. Comparison of the frequency responses of the primary system: ———, overall level; ——, fundamental harmonic.

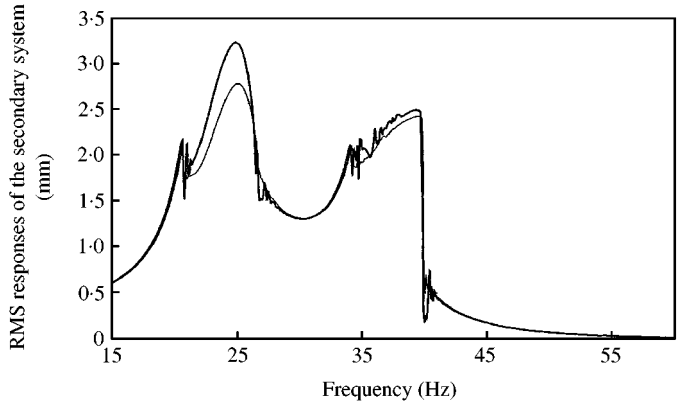

Figure 17. Comparison of the frequency response of the secondary system: ———, overall level; ——, fundamental harmonic.

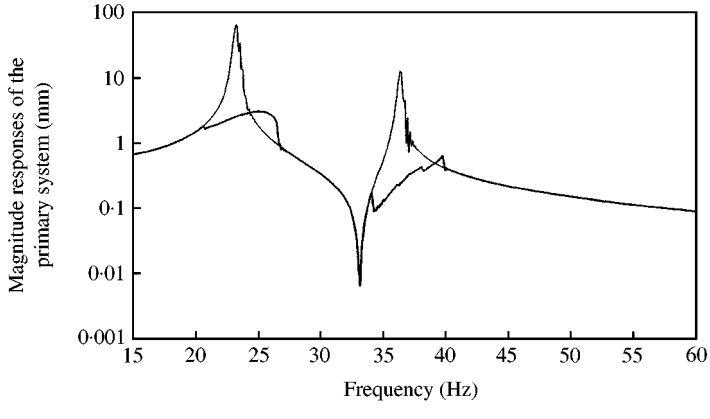

Figure 18. Comparison of the fundamental harmonics of displacement of the primary system in the linear case (——) and vibroimpact case (———).

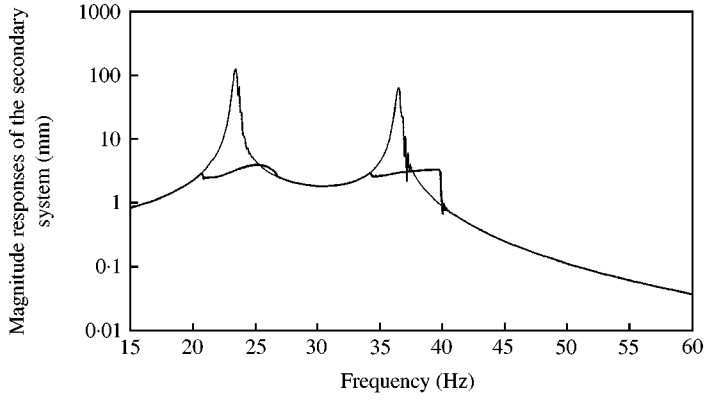

Figure 19. Comparison of the fundamental harmonics of displacement of the secondary system in the linear case (——) and vibroimpact case (———).

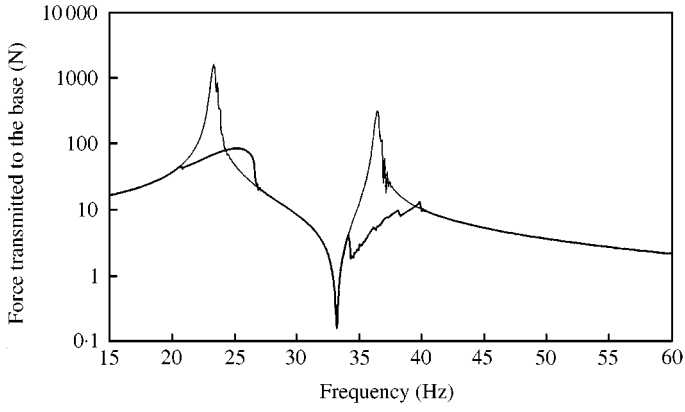

Figure 20. Comparison of the fundamental harmonics of the force transmitted to the base in the linear case (– – –) and vibro-impact case (———).

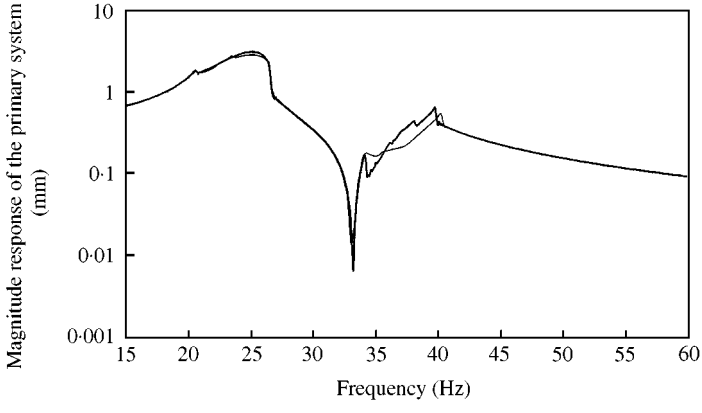

Figure 21. Comparison of the fundamental harmonics of displacement of the primary system: simulation (– – –) versus PGF analytical solution (———).

correction of the frequency responses in the vicinities of linear resonances. At the same time, the deep linear anti-resonant notch remains unaffected.

Figures 21–23 compare the magnitudes of fundamental harmonics of the frequency responses of the primary and secondary systems and the force transmitted to the base which are obtained by means of the analytical method of PGF, with that obtained by numerical simulation. It is seen that the results obtained are in a good agreement. Figure 24 shows the comparison of the dependencies of impact impulses against frequency obtained by the PGF method with those obtained by numerical simulation. Once again, the results are in fair agreement.

6. DESIGN CONCEPTS

6.1. INFLUENCE OF RESTITUTION RATIO

With the use of the analytical solution obtained, one can estimate the influence of the restitution ratio, R, on the performance of the vibration protection system. Figure 25 shows

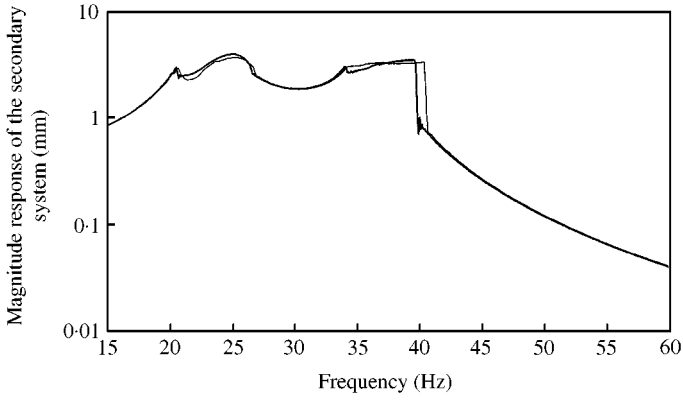

Figure 22. Comparison of the fundamental harmonics of displacement of the secondary system: simulation (——) versus PGF analytical solution (– – –).

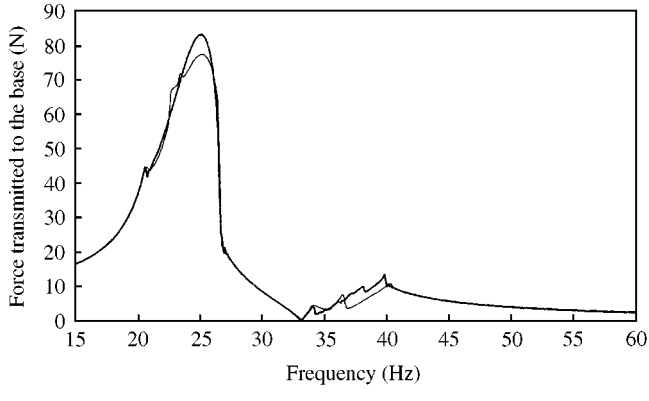

Figure 23. Comparison of the fundamental harmonics of the force transmitted to the base: simulation (——) versus PGF analytical solution (– – –).

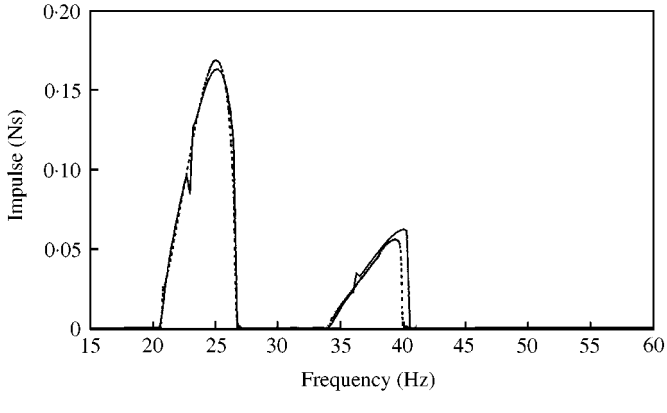

Figure 24. Comparison of the impact impulses: simulation (- - -) versus PGF analytical solution (——).

the dependence of the peak magnitudes of the fundamental harmonic of deflection of the primary system on the restitution ratio at the constant clearance $\Delta = 3$ mm. The analytical results (dashed curve) are compared with the numerical simulation (solid curve). In the numerical simulation, the dependence $R(\xi_b)$ in Figure 14 was used for the calculation of the

bumper loss factor ξ_b. The apparent natural frequency of the bumper was taken as $\Omega_b/2\pi = 250$ Hz. The results of numerical simulation and analytical calculation are in good agreement and indicate the usefulness of the low restitution ratio at impact for the quality of vibration protection systems. As seen from Figure 25, the further decrease of the restitution ratio below the value of $R = 0{\cdot}2$ ($\xi_b = 0{\cdot}65$) becomes ineffective.

6.2. INFLUENCE OF CLEARANCE

Following the previous analysis, it is useful to estimate the influence of the clearance Δ on the entire performance of the vibration protection system. Figure 26 shows the dependence of the peak magnitude of the fundamental harmonic against the clearance at the constant restitution ratio $R = 0{\cdot}2$. The analytical results (dashed line) are compared with the numerical simulation (solid line). The apparent natural frequency of the bumper was $\Omega_b/2\pi = 250$ Hz. The results of numerical simulation and analytical results are in good agreement and indicate the usefulness of the low clearance for the quality of a vibration protection system. It is evident that the value of the clearance is limited from below by the

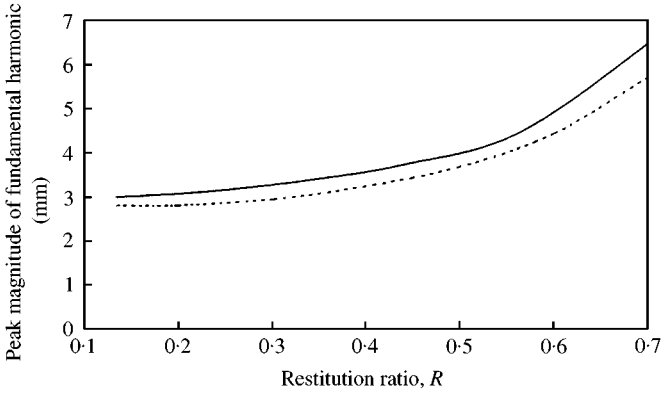

Figure 25. Peak displacement magnitude of the primary system at different restitution ratios: simulation (——) versus PGF analytical solution: (- - - -).

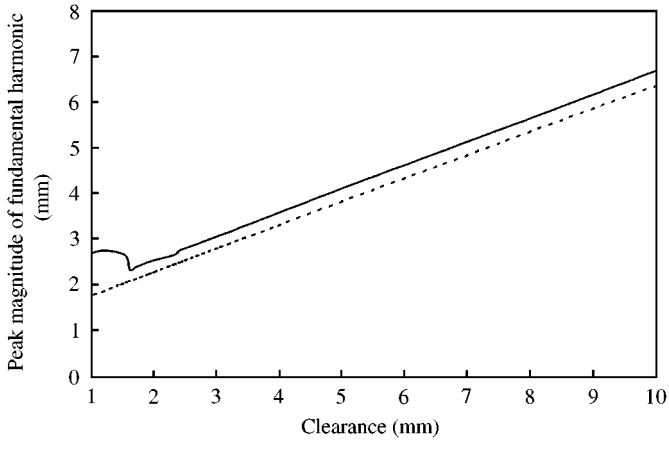

Figure 26. Peak displacement magnitude of the primary system at different clearances: simulation (——) versus PGF analytical solution: (- - - -).

value of the impactless amplitude of the secondary system at antiresonant frequency and the desirable width of the frequency span of impactless operation of the vibration protection system (see also Figures 2 and 4).

6.3. CALCULATION OF PEAK ACCELERATIONS

It was indicated above that consideration of momentary impact does not allow for the estimation of the peak values of impact accelerations. Nevertheless, for the practical design of the bumper these values are of significant importance.

The combination of the method of PGF with the theory of viscoelastic impact developed in reference [5–7] allows an approximate estimation of the values of impact peak accelerations.

With reference to formula (9), the value of pre-impact velocity may be calculated as

$$\dot{X}_2(-0) = J/M_2(1 + R).$$

From references [5, 7], the peak value of acceleration at visco-elastic impact may be expressed in terms of the pre-impact velocity $\dot{X}_2(-0)$, apparent natural frequency of the bumper Ω_b and the function $\Gamma(\xi_b)$, as

$$Apeak = \dot{X}_2(-0)\Omega_b\Gamma(\xi_b),$$

where

$$\Gamma(\xi_b) = \begin{cases} \gamma(\xi_b) & \text{if } \gamma(\xi_b) \geqslant 2\xi_b \\ 2\xi_b & \text{if } \gamma(\xi_b) < 2\xi_b \end{cases}$$

and

$$\gamma(\xi_b) = \frac{1}{\xi_b(3-4\xi_b^2)} \exp\left[-\frac{\xi_b}{\sqrt{1-\xi_b^2}} \operatorname{atan} \frac{(4\xi_b^2-1)\sqrt{1-\xi^2}}{\xi_b(3-4\xi_b^2)}\right] \cos\left[\operatorname{atan} \frac{(4\xi_b^2-1)\sqrt{1-\xi_b^2}}{\xi_b(3-4\xi_b^2)}\right].$$

By using the dependencies $R = R(\xi_b)$ from equation (26) and $\Gamma = \Gamma(\xi_b)$ one can construct the dependencies $\xi_b(R)$ and $\Psi(R) = \Gamma[\xi_b(R)]$ (see Figure 27). Finally one obtains

$$Apeak = \frac{J\Omega_b\Psi(R)}{M_2(1 + R)}.$$

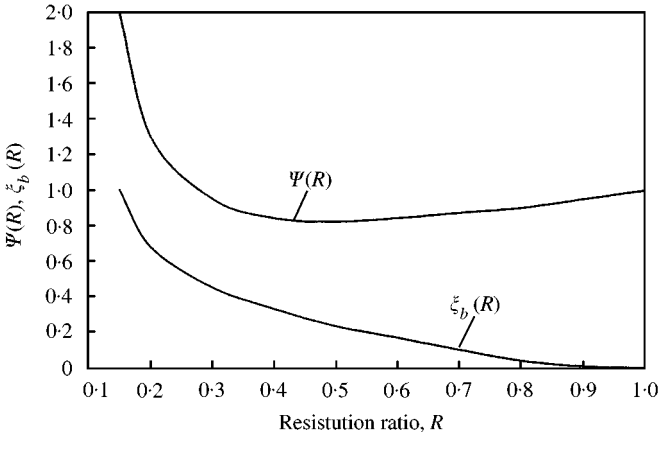

Figure 27. Functions $\Psi(R)$, $\xi_b(R)$.

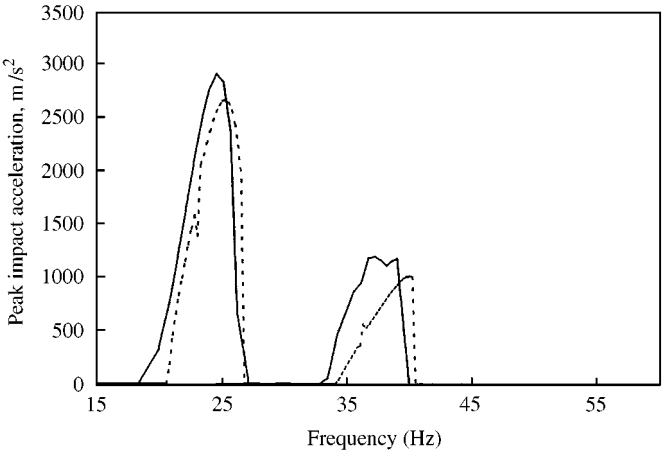

Figure 28. Peak impact accelerations at different frequencies: simulation (——) versus PGF analytical solution: (- - - -).

Figure 28 shows the results of direct numerical simulation of the peak values of acceleration against the excitation frequency for the system with the clearance $\Delta = 3$ mm and the bumper with $\Omega_b/2\pi = 250$ Hz and $\xi_b = 0{\cdot}65$ (solid line). The peak values of accelerations against the excitation frequency were also calculated by using the latter formula for the system with the same clearance and restitution ratio $R = 0{\cdot}2$ (dashed line). The values of the impact impulses J were calculated by means of the PGF method. It was considered again that $\Omega_b/2\pi = 250$ Hz. The agreement is evident.

7. CONCLUSIONS

The vibration protection system which relies on the undamped tuned dynamic absorber was investigated. The correction of the extraneous frequency response of such a system at resonant frequencies without affecting the ability of sufficient linear vibration suppression at anti-resonant frequency was achieved due to the limiting of the motion of the secondary system by means of a bumper mounted upon the foundation.

The exact solution to the problem was obtained with the use of the theory of momentary impact and the technique of periodic Green functions and contains a full set of harmonics. This solution was compared with numerical simulation which relies on the realistic model of visco-elastic impact. The results were in fair agreement.

Recommendations for a practical design of such a vibration protection system were made.

REFERENCES

1. J. ORMONDROYD and J. P. DEN HARTOG 1928 *Transactions of ASME* **50**, 9–22. The theory of the dynamic vibration absorber.
2. S. TIMOSHENKO 1955 *Vibration Problems in Engineering*. New York: D. Van Nostrand Company.
3. S. F. MASRI 1972 *International Journal of Non-Linear Mechanics* **7**, 663–675. Forced vibration of a class of nonlinear two-degree-of freedom oscillators.
4. D. H. GONSALVES, R. D. NEILSON and A. D. S. BARR 1993 *Journal of Mechanical Engineering Science* **207**, 363–374. The dynamics and design of a non-linear vibration absorber.
5. V. I. BABITSKY 1998 *Theory of Vibro-impact Systems and Applications*. Berlin: Springer-Verlag. Revised translation from Russian. Moscow: Nauka, 1978.
6. S. A. KEMBER and V. I. BABITSKY 1999 *Journal of Sound and Vibration* **227**, 427–447. Excitation of vibro-impact systems by periodic impulses.
7. V. I. BABITSKY and A. M. VEPRIK 1998 *Journal of Sound and Vibration* **218**, 269–292. Universal bumpered vibration isolator for severe environment.